

## Vibrational spectroscopic studies and computational study of 4-fluoro-N-(2'-hydroxy-4'-nitrophenyl)phenylacetamide

Y. Sheena Mary<sup>a,c,\*</sup>, C. Yohannan Panicker<sup>b,1</sup>, Hema Tresa Varghese<sup>c,1</sup>, K. Raju<sup>a</sup>, Tugba Ertan Bolelli<sup>d</sup>, Ilkay Yildiz<sup>d</sup>, Carlos M. Granadeiro<sup>e</sup>, Helena I.S. Nogueira<sup>e</sup>

<sup>a</sup> Department of Physics, University College, Trivandrum, Kerala, India

<sup>b</sup> Department of Physics, TKM College of Arts and Science, Kollam, Kerala, India

<sup>c</sup> Department of Physics, Fatima Mata National College, Kollam, Kerala, India

<sup>d</sup> Faculty of Pharmacy, Department of Pharmaceutical Chemistry, Ankara University, Tandogan 06100, Ankara, Turkey

<sup>e</sup> Department of Chemistry, CICECO, University of Aveiro, 3810-193 Aveiro, Portugal

### ARTICLE INFO

#### Article history:

Received 28 December 2010

Received in revised form 8 March 2011

Accepted 8 March 2011

Available online 12 March 2011

#### Keywords:

Acetamide

FT-IR

FT-Raman

DFT calculations

SERS

### ABSTRACT

Fourier-transform infrared (FT-IR) and FT-Raman spectra of 4-fluoro-N-(2'-hydroxy-4'-nitrophenyl)phenylacetamide were recorded and analyzed. A surface-enhanced Raman scattering (SERS) spectrum was recorded in silver colloid. The vibrational wavenumbers and corresponding vibrational assignments were examined theoretically using quantum mechanical calculations. The red shift of the NH stretching wavenumber in the IR spectrum from the calculated wavenumber indicates the weakening of NH bond resulting in proton transfer to the neighboring oxygen atom. The presence of CH<sub>2</sub> and NO<sub>2</sub> modes in the SERS spectrum indicates the nearness of these groups to the metal surface, which affects the orientation and metal molecule interaction. The presence of phenyl ring deformation bands, show a tilted orientation of the molecule with respect to the silver surface. The first hyperpolarizability and predicted infrared intensities are reported. The calculated first hyperpolarizability is comparable with the reported values of similar structures and is an attractive object for further studies of nonlinear optics.

© 2011 Elsevier B.V. All rights reserved.

### 1. Introduction

N-Phenyl benzamides are important and biologically active compounds [1]. Some N-(o-hydroxyphenyl)benzamides and phenylacetamides have been reported as possible metabolites of antimicrobial active benzoxazoles. Synthesis and microbiological activity of some N-(2-hydroxy-4-substitutedphenyl)benzamides, phenylacetamides and furamides as possible metabolites of antimicrobial active benzoxazoles are reported by Aki-Sener et al. [2]. Benzamide derivatives which are the possible metabolites of benzoxazoles show various type of biological properties such as antihelminthic, antihistaminic, antifungal and antibacterial [1]. Vibrational spectroscopic studies and DFT calculations of 4-fluoro-N-(2'-hydroxy-4'-nitrophenyl) benzamide was reported by Ushakumari et al. [3]. The intra molecular hydrogen bond in 2-hydroxy-benzamides are reported by Kawski et al. [4]. Arslan et al. [5] reported the molecular structure and vibrational spectra of 2-chloro-N-(diethylcarbamothioyl)benzamide by Hartree–Fock and density

functional methods. Gas phase structures of fundamental amides, formamide [6] and acetamide [7] were determined by electron diffraction and their crystal structures were studied by X-ray and neutron diffraction [8–12]. The crystal structures of benzamide were determined by X-ray [13] and neutron diffraction [14]. Near infrared spectroscopic studies of the hydrogen bonding between thioacetamide and N,N-disubstituted benzamide derivatives in CCl<sub>4</sub> is reported by Choi et al. [15]. Molecular structure benzamide was studied by gas phase electron diffraction [16]. Biagi et al. [17] reported the synthesis and biological activity of novel substituted benzanilides as potassium channel activators. Rho et al. [18] reported the studies on depigmenting activities of dihydroxyl benzamide derivatives containing adamantane moiety. DFT and ab initio study of structure of dyes derived from 2-hydroxy and 2,4-hydroxy benzoic acids are reported by Dabbagh et al. [19] Nishikawa et al. [20] reported the internal rotations of aromatic polyamides theoretically. In the present work, the IR, Raman, SERS and theoretical calculations of the wavenumbers for the title compound are reported. Nonlinear optics deals with the interaction of applied electromagnetic fields in various materials to generate new electromagnetic fields, altered in wavenumber, phase, or other physical properties [21]. Organic molecules able to manipulate photonic signals efficiently are of importance in technologies such as optical communication, optical computing, and dynamic

\* Corresponding author at: Department of Physics, University College, Trivandrum, Kerala, India.

E-mail address: [sypanicker@rediffmail.com](mailto:sypanicker@rediffmail.com) (Y.S. Mary).

<sup>1</sup> Temporary address: Department of Physics, Mar Ivanios College, Nalanchira, Trivandrum, Kerala, India.

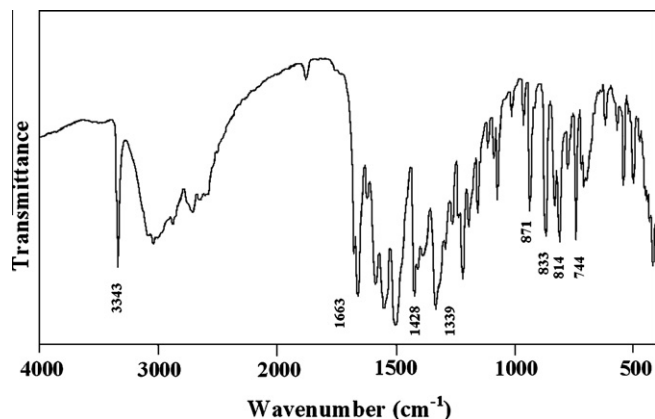


Fig. 1. FTIR spectrum of 4-fluoro-N-(2-hydroxy-4-nitrophenyl)phenylacetamide.

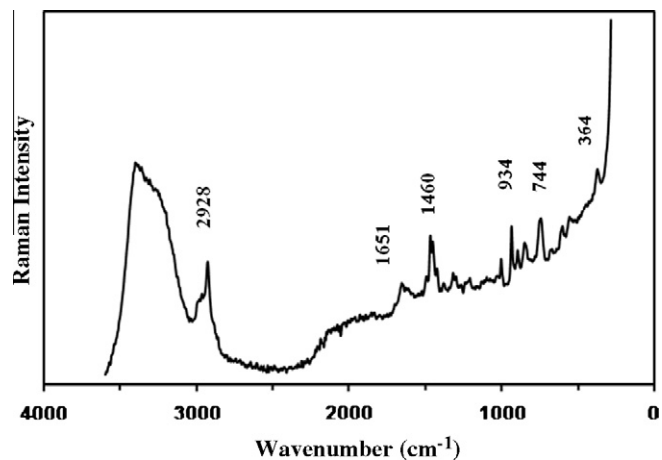


Fig. 3. SERS spectrum of 4-fluoro-N-(2-hydroxy-4-nitrophenyl)phenylacetamide.

image processing [22,23]. Phenyl substituents can increase molecular hyperpolarizability [24,25] a result described as surprising. Many organic molecules, containing conjugated  $\pi$  electrons and characterized by large values of molecular first hyperpolarizabilities, were analyzed by means of vibrational spectroscopy [26]. In this context, the hyperpolarizability of the title compound is calculated in the present study.

## 2. Experimental

The chemicals were purchased from the commercial vendors and were used without purification. The reactions were monitored and the purity of the product was checked by thin layer chromatography (TLC). Silica gel 60 F<sub>254</sub> chromatoplates were used for TLC. The solvent systems were chloroform/methanol (15:1). Thionyl chloride (1.5 ml) and 4-fluorophenyl acetic acid (0.5 mmol) were refluxed in benzene (5 ml) at 80° for 3 h, and then excess thionyl chloride was removed in vacuo [27]. The residue was dissolved in ether (10 ml) and the solution added during 1 h to a stirred, ice-cold mixture of 2-amino-5-nitrophenol (0.5 mmol), sodiumbicarbonate (0.5 mmol), diethyl ether (10 ml), and water (10 ml). The mixture was stirred overnight at room temperature and filtered. After the precipitate was washed with water, 2 N HCl and water, respectively, and finally with ether, compound was obtained. The crude product was purified by recrystallization from ethanol.

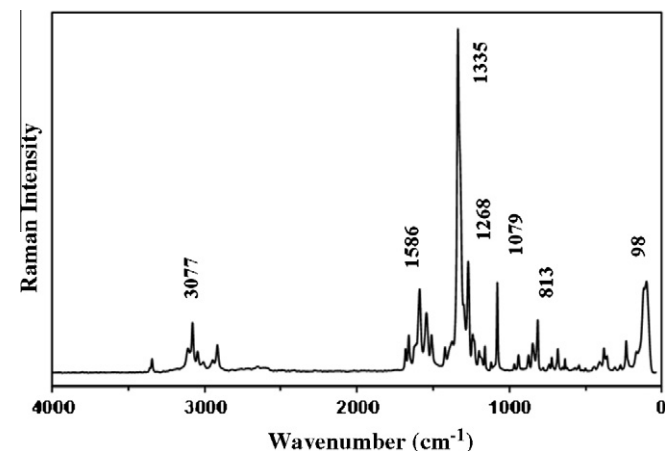


Fig. 2. FT-Raman spectrum of 4-fluoro-N-(2-hydroxy-4-nitrophenyl)phenylacetamide.

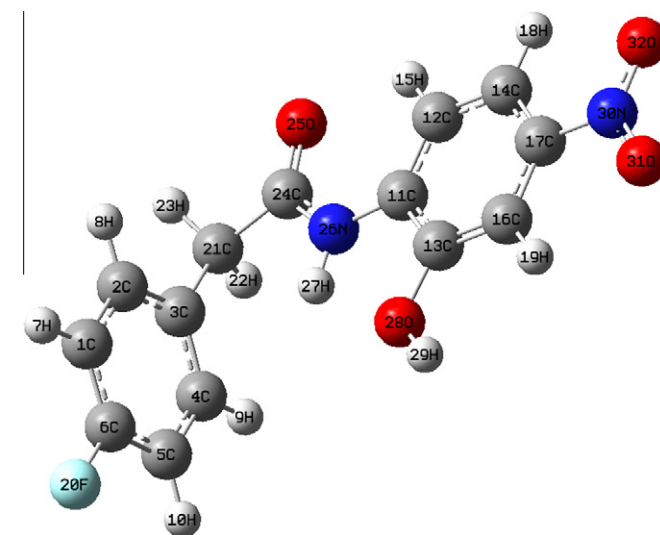


Fig. 4. Optimized geometry of 4-fluoro-N-(2-hydroxy-4-nitrophenyl)phenylacetamide.

The purity of the compound was checked by TLC (Merck TLC plates Silica gel 60 F<sub>254</sub>) using solvents S1 (CHCl<sub>3</sub>/MeOH 15:1). The plates were visualized using UV light. Melting points (uncorrected) was determined using a capillary melting point apparatus (Buchi SMP 20 and Electrothermal 9100): 226–228 °C. Yield was calculated after recrystallization. Yield 33%. The IR spectrum (Fig. 1) was recorded on a Jasco FT-IR-420 spectrometer with KBr disks. The FT-Raman spectra (Figs. 2 and 3) was obtained on a Bruker RFS 100/S, Germany. For excitation of the spectrum, the emission of a Nd:YAG laser was used, excitation wavelength 1064 nm, maximal power 150 mW, measurement on solid sample. The aqueous silver colloid used in the SERS experiments was prepared by reduction of silver nitrate by sodium citrate, using the Lee-Meisel method [28]. Solutions of the title compound were made up in ethanol (0.1 mmol in 1 cm<sup>3</sup> of solvent) and transferred by a microsyringe into the silver colloid (10  $\mu$ L in 1 cm<sup>3</sup> of colloid) such that the overall concentration was 10<sup>-3</sup> mol dm<sup>-3</sup>. Colloid aggregation was induced by addition of an aqueous solution of MgCl<sub>2</sub> (1 drop of a 2 mol dm<sup>-3</sup> solution). Polyvinylpyrrolidone was then used to stabilize the colloid (1 drop of 0.1 g/10 cm<sup>3</sup> aqueous solution). The final colloid mixture was placed in a glass tube and the Raman spectrum registered.

The <sup>1</sup>H NMR spectra was recorded employing a VARIAN Mercury 400 MHz FT spectrometer, chemical shifts ( $\delta$ ) are in

ppm relative to TMS, and coupling constants ( $J$ ) are reported in Hertz. Elemental analysis was taken on a Leco 932 CHNS–O analyzer. The results of the elemental analysis (C, H, N) was within  $\pm 0.4\%$  of the calculated amounts. Elemental analyses: calculated: C, 57.93; H, 3.82; N, 9.65; found: C, 57.68; H, 3.87; N, 9.649.  $^1\text{H}$  NMR ( $\text{DMSO-d}_6$ )  $\delta$  ppm,  $J = \text{Hz}$ : 3.83 (s, 2H,  $\text{CH}_2$ ); 7.08–7.18 (m, 2H, 3–H, 5–H); 7.35–7.40 (m, 2H, 2–H, 6–H); 7.65–7.71 (m, 2H, 3'–H, 5'–H); 8.26 (d, 1H,  $J_0 = 8.8$ , 6'–H); 9.67 (s, 1H, OH); 11.09 (s, 1H, NH).

### 3. Computational details

The vibrational wavenumbers were calculated using the Gaussian03 software package on a personal computer [29]. The computations were performed at HF/6-31G\*, B3PW91/6-31G\* and B3LYP/6-31G\* levels of theory to get the optimized geometry (Fig. 4) and vibrational wavenumbers of the normal modes of the title compound. Parameters corresponding to optimized geometry of the title compound are given in Table S1 (Supporting information). The DFT partitions, the electronic energy  $E = E_T + E_V + E_J + E_{XC}$ , where  $E_T$ ,  $E_V$  and  $E_J$  are electronic kinetic energy, electron nuclear attraction and electron–electron repulsion terms, respectively. The electron correlation is taken into account in the DFT via the exchange–correlation term  $E_{XC}$ , which includes exchange energy arising from the anti-symmetry of quantum mechanical wave function and dynamic correlation in the motion of individual electron, and it makes DFT dominant over conventional HF procedure [30]. DFT calculations were carried out with Becke's three-parameter hybrid model using the Lee–Yang–Parr correlation functional (B3LYP) method. Molecular geometries were fully optimized by Berny's optimization algorithm using redundant internal coordinates. Harmonic vibrational wavenumbers were calculated using analytic second derivatives to confirm the convergence to minima in the potential surface. At the optimized structure of the examined species, no imaginary wavenumber modes were obtained, proving that a true minimum on the potential surface was found. The optimum geometry was determined by minimizing the energy with respect to all geometrical parameters without imposing molecular symmetry constraints. The DFT hybrid B3LYP functional tends also to overestimate the fundamental modes; therefore scaling factors have to be used for obtaining a considerably better agreement with experimental data [31]. Scaling factors 0.9613 and 0.8929 has been uniformly applied for the DFT and HF calculated wavenumbers

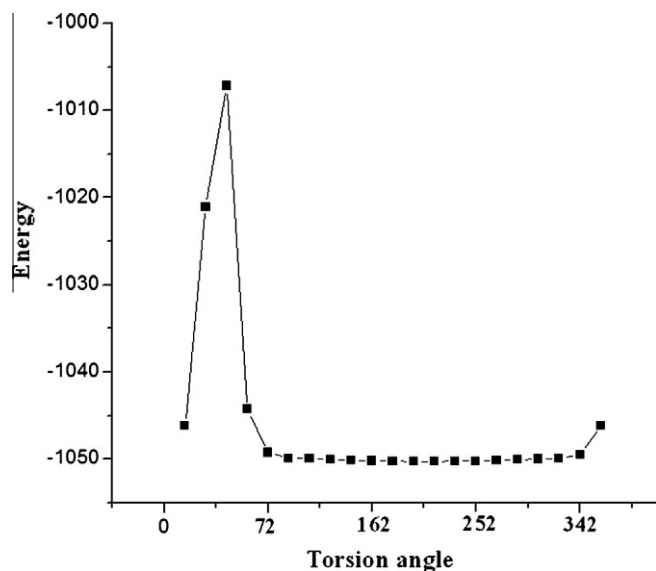


Fig. 5. Profile of potential energy scan for the torsion angle  $\text{O}_{25}\text{--C}_{24}\text{--C}_{21}\text{--C}_3$ .

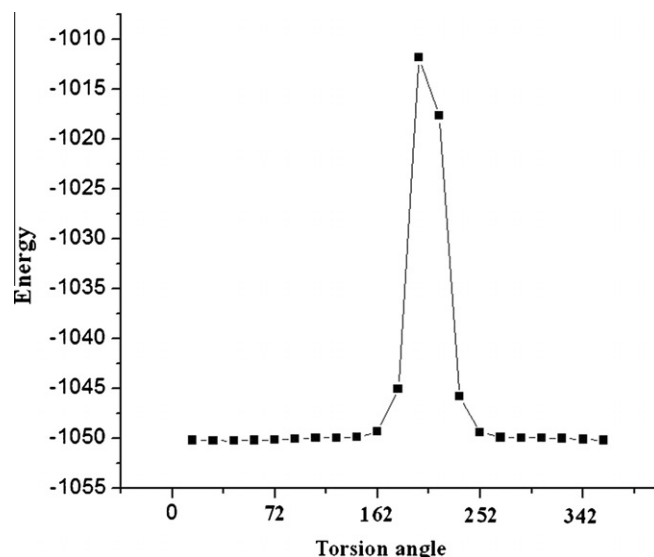


Fig. 6. Profile of potential energy scan for the torsion angle  $\text{N}_{26}\text{--C}_{24}\text{--C}_{21}\text{--C}_3$ .

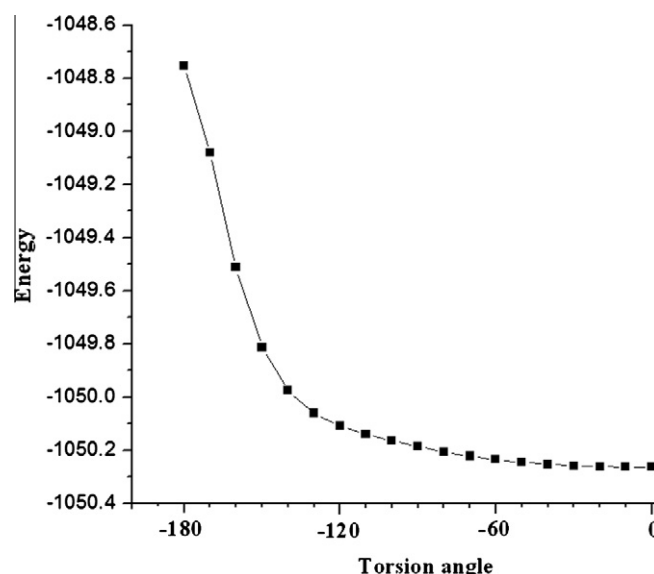


Fig. 7. Profile of potential energy scan for the torsion angle  $\text{H}_{27}\text{--N}_{26}\text{--C}_{24}\text{--C}_{21}$ .

[30]. The observed disagreement between theory and experiment could be a consequence of the anharmonicity and of the general tendency of the quantum chemical methods to overestimate the force constants at the exact equilibrium geometry [32]. The assignments of the calculated wavenumbers are aided by the animation option of MOLEKEL program, which gives a visual presentation of the vibrational modes [33,34]. Potential energy surface scan studies has been carried out to understand the stability of planar and non-planar structures of the molecule. The profiles of potential energy surface for torsion angles  $\text{O}_{25}\text{--C}_{24}\text{--C}_{21}\text{--C}_3$ ,  $\text{N}_{26}\text{--C}_{24}\text{--C}_{21}\text{--C}_3$  and  $\text{H}_{27}\text{--N}_{26}\text{--C}_{24}\text{--C}_{21}$  are given in Figs. 5–7. The energy is minimum for  $-153.7^\circ$  ( $-1050.26281$  Hartree),  $28.8^\circ$  ( $-1050.26130$  Hartree) and  $-4.5^\circ$  ( $-1050.26271$  Hartree) for the torsion angles.

## 4. Results and discussion

### 4.1. IR and Raman spectra

The observed IR, Raman bands with the relative intensities and calculated (scaled) wavenumbers and assignments are given in

**Table 1.** Fluorine atoms directly attached to the aromatic ring give rise bands [35] in the region 1100–1270  $\text{cm}^{-1}$ . Many of these compounds [35] including the simpler ones with one fluorine only on the ring, absorb near 1230  $\text{cm}^{-1}$ . The  $\nu\text{C}-\text{F}$  is reported at 1157, 1233  $\text{cm}^{-1}$  (IR), 1244  $\text{cm}^{-1}$  (HF) [36,37]. For the title compound, the band observed at 1225  $\text{cm}^{-1}$  in the IR spectrum is assigned as  $\nu\text{C}-\text{F}$  mode. The DFT calculations give this mode at 1218  $\text{cm}^{-1}$ . The substitution of fluorine in the phenyl ring changes the C–C bond lengths  $\text{C}_1-\text{C}_6$  and  $\text{C}_5-\text{C}_6$  of the benzene ring. Fluorine is highly electronegative and thus to obtain additional electron density it attempts to draw it from the neighbouring atoms, which move closer together in order to share the remaining electrons more easily as a result. Due to this, the bond angle A(1,6,5) is found to be 122.4° in the present case, which is 120° for normal benzene. Similarly, the bond lengths  $\text{C}_1-\text{C}_6$  and  $\text{C}_5-\text{C}_6$  are 1.3920 Å and 1.3895 Å, respectively, while for normal benzene it is 1.3864 Å [37].

The vibrations of the  $\text{CH}_2$  group (the asymmetric stretch  $\nu_{\text{as}}\text{CH}_2$ , symmetric stretch  $\nu_{\text{s}}\text{CH}_2$ , scissoring vibrations  $\delta\text{CH}_2$  and the wagging vibration  $\omega\text{CH}_2$ ) appears in the regions 2940  $\pm$  20, 2885  $\pm$  45, 1440  $\pm$  10 and 1340  $\pm$  25  $\text{cm}^{-1}$ , respectively [35,38]. These bands are observed at 2942  $\text{cm}^{-1}$  in the IR spectrum, 2992, 2927  $\text{cm}^{-1}$  in the Raman spectrum and at 2999, 2938, 1456, 1301  $\text{cm}^{-1}$  theoretically for the title compound. The twisting and rocking modes of the  $\text{CH}_2$  group appear in the regions [38] 1260  $\pm$  10 and 800  $\pm$  25  $\text{cm}^{-1}$ . These modes are also assigned (Table 1).

The C=O stretching vibrations [38,39] are expected in the region 1715–1680  $\text{cm}^{-1}$  and in the present study this mode appears at 1663  $\text{cm}^{-1}$  in IR and 1658  $\text{cm}^{-1}$  in Raman spectrum. The DFT calculations give this mode at 1639  $\text{cm}^{-1}$ . El-Shahawy et al. [40] reported a value 1640  $\text{cm}^{-1}$  in the IR spectrum as  $\nu\text{C}=\text{O}$  for paracetamol. The  $\delta\text{C}=\text{O}$  in-plane deformation [38] has been found in the region 625  $\pm$  70  $\text{cm}^{-1}$  and the band at 638  $\text{cm}^{-1}$  in Raman spectrum and 641  $\text{cm}^{-1}$  in (DFT) is assigned as this mode. The C=O out-of-plane deformation [38] is in the range 540  $\pm$  80  $\text{cm}^{-1}$ , and the DFT calculations give this mode at 486  $\text{cm}^{-1}$  and weak bands are observed at 499  $\text{cm}^{-1}$  in IR and at 484  $\text{cm}^{-1}$  in the Raman spectrum.

The NH stretching vibration appears strongly and broadly in the region [38] 3390  $\pm$  60  $\text{cm}^{-1}$ . For the title compound the strong band at 3343  $\text{cm}^{-1}$  in the IR spectrum and 3340  $\text{cm}^{-1}$  in Raman spectrum is assigned as  $\nu\text{NH}$  mode. The calculated value for this mode is 3433  $\text{cm}^{-1}$ . The NH stretching wavenumber is red shifted by 90  $\text{cm}^{-1}$  in the IR spectrum with a strong intensity from the computed wavenumber, which indicates the weakening of the N–H bond resulting in proton transfer to the neighboring oxygen [39]. The CNH vibration in which N and H atoms move in opposite direction of carbon atom in the amide moiety appears at 1497  $\text{cm}^{-1}$  theoretically, and the CNH vibration in which N and H atoms move in the same direction of carbon atom in the amide group appears at 1217 (DFT) [35,40,41]. The NH rock in the plane observed at 1162 (IR), 1158 (Raman) and at 1166  $\text{cm}^{-1}$  theoretically [40]. The out-of-plane wagging [38] of NH is moderately active with a broad band in the region 790  $\pm$  70  $\text{cm}^{-1}$  and the band 763  $\text{cm}^{-1}$  (DFT) is assigned as this mode. El-Shahawy et al. [40] reported a value 720  $\text{cm}^{-1}$  for this mode. The C–N stretching vibration [38] coupled with  $\delta\text{NH}$ , is moderately to strongly active in the region 1275  $\pm$  55  $\text{cm}^{-1}$ . El-Shahawy et al. [40] observed a band at 1320  $\text{cm}^{-1}$  in the IR spectrum as this  $\nu\text{C}-\text{N}$  mode. In the present case, the band at 1339  $\text{cm}^{-1}$  in the IR spectrum and 1335  $\text{cm}^{-1}$  in Raman spectrum is assigned as this mode. The DFT calculations give the corresponding band at 1325  $\text{cm}^{-1}$ .

The OH group provides three normal vibrations  $\nu\text{OH}$ ,  $\delta\text{OH}$  and  $\gamma\text{OH}$ . The DFT calculations give the  $\nu\text{OH}$  band at 3556  $\text{cm}^{-1}$ . The in-plane OH deformation [38] is expected in the region 1400  $\pm$  40  $\text{cm}^{-1}$  and the band at 1428  $\text{cm}^{-1}$  (IR) and 1432  $\text{cm}^{-1}$  (DFT) are assigned as this mode, which is not pure but contains sig-

nificant contribution from phenyl ring stretching modes. The stretching of the hydroxyl group with respect to the phenyl moiety  $\nu(\text{C}-\text{O})_h$  appears at 1270  $\text{cm}^{-1}$  in the IR spectrum, 1268  $\text{cm}^{-1}$  in Raman spectrum and the calculated value is 1261  $\text{cm}^{-1}$ . This band is expected [35,41,42] in the region 1220  $\pm$  40  $\text{cm}^{-1}$ . The out-of-plane OH deformation is observed at 621  $\text{cm}^{-1}$  in the IR spectrum and at 612  $\text{cm}^{-1}$ , theoretically, which is expected [38] in the region 650  $\pm$  80  $\text{cm}^{-1}$ . For paracetamol,  $\nu(\text{C}-\text{O})_h$  and  $\gamma\text{OH}$  are reported at 1240 and 620  $\text{cm}^{-1}$ , respectively [40].

The most characteristic bands in the spectrum of nitro compounds are due to  $\text{NO}_2$  stretching, which are the two most useful group wavenumbers, not only because of their spectral position but also for their strong intensity [38]. In nitro compounds the anti-symmetric  $\text{NO}_2$  stretching vibrations [38] are located in the region 1580  $\pm$  80  $\text{cm}^{-1}$ . The symmetric  $\text{NO}_2$  stretching vibrations [38] are expected in the region 1380  $\pm$  20  $\text{cm}^{-1}$ . In substituent nitrobenzenes,  $\nu_{\text{s}}\text{NO}_2$  appears strongly at 1345  $\pm$  30  $\text{cm}^{-1}$ , in 3-nitropyridine [43] at 1330  $\pm$  20  $\text{cm}^{-1}$ , and in conjugated nitroalkenes [44] at 1345  $\pm$  15  $\text{cm}^{-1}$ . In the present case the bands observed at 1555  $\text{cm}^{-1}$  in the IR spectrum and 1534  $\text{cm}^{-1}$  in the Raman spectrum are assigned as asymmetric  $\text{NO}_2$  modes. The  $\nu_{\text{s}}\text{NO}_2$  mode is observed at 1391  $\text{cm}^{-1}$  in the IR spectrum. The DFT calculations give 1527 and 1396  $\text{cm}^{-1}$  as asymmetric and symmetric  $\text{NO}_2$  stretching modes respectively. According to some investigators [45–47] the  $\text{NO}_2$  scissors [38] occur in the region 850  $\pm$  60  $\text{cm}^{-1}$  when conjugated to C= or aromatic molecules, with a contribution of the  $\nu\text{CN}$ , which is expected to be near 1120  $\text{cm}^{-1}$ . For nitrobenzene,  $\delta\text{NO}_2$  is reported at [38] 852  $\text{cm}^{-1}$ , for  $\text{H}_2\text{C}=\text{CHNO}_2$  at 890  $\text{cm}^{-1}$ , and for 1,3-dinitrobenzene at 904 and 834  $\text{cm}^{-1}$ . For the title compound, the DFT calculations give the band at 862  $\text{cm}^{-1}$  as the deformation band of  $\text{NO}_2$ . The band observed at 869  $\text{cm}^{-1}$  in Raman spectrum is assigned as  $\delta\text{NO}_2$ . In aromatic compounds, the wagging mode  $\omega\text{NO}_2$  is observed at 740  $\pm$  50  $\text{cm}^{-1}$  with a moderate to strong intensity, a region in which  $\gamma\text{CH}$  is also active [38].  $\omega\text{NO}_2$  is reported at 701 and 728  $\text{cm}^{-1}$  for 1,2-dinitrobenzene and at 710 and 772  $\text{cm}^{-1}$  for 1,4-dinitrobenzene [38]. For the title compound, the band at 744  $\text{cm}^{-1}$  in the IR spectrum, 759  $\text{cm}^{-1}$  in the Raman spectrum and 762  $\text{cm}^{-1}$  (DFT) is assigned as  $\omega\text{NO}_2$  mode. In aromatic compounds, the rocking mode  $\rho\text{NO}_2$  is active in the region 545  $\pm$  45  $\text{cm}^{-1}$ . Nitrobenzene [38] shows this rocking mode at 531  $\text{cm}^{-1}$ . In the present case the DFT calculations give this rocking mode of  $\text{NO}_2$  533  $\text{cm}^{-1}$ . Sundaraganesan et al. [48] reported the  $\text{NO}_2$  deformation bands at 839, 744 and 398  $\text{cm}^{-1}$  (experimentally) and at 812, 716, 703 and 327  $\text{cm}^{-1}$  theoretically.

Since the identification of all the normal modes of vibration of large molecules is not trivial, we tried to simplify the problem by considering each molecule as a substituted benzene. Such an idea has already been successfully utilized by several workers for the vibrational assignments of molecules containing multiple homo and hetero aromatic rings [37]. In the following discussion, the tri-substituted and para substituted phenyl rings are designated as ring I and II, respectively. The modes in the two phenyl rings will differ in wavenumber and the magnitude of splitting will depend on the strength of interaction between different parts (internal coordinates) of the two rings. For some modes, this splitting is so such that they may be considered as quasi-degenerate, and for other modes a significant amount of splitting may be observed [37]. The aromatic CH stretching vibrations [38] absorb weakly to moderately between 3120 and 3000  $\text{cm}^{-1}$ . The B3LYP calculations give bands in the range 3077–3160  $\text{cm}^{-1}$  as  $\nu\text{CH}$  stretching modes of the phenyl rings. Experimentally, we have observed bands at 3113, 3046  $\text{cm}^{-1}$  in the IR spectrum and at 3087, 3077, 3039  $\text{cm}^{-1}$  in the Raman spectrum as  $\nu\text{CH}$  modes. The benzene ring possesses six ring stretching vibrations of which the four with the highest wavenumbers occurring near 1600, 1580, 1490 and 1440  $\text{cm}^{-1}$  are good group vibrations [38]. With heavy substitu-

**Table 1**  
Calculated vibrational wavenumbers (scaled), measured infrared and Raman band positions and assignments for 4- $\tau$ -N-(2-hydroxy-4-nitrophenyl)phenylacetamide.

HF/6-31G*		B3PW91/6-31G*		B3LYP/6-31G*		$\nu_{(IR)}$ (cm <sup>-1</sup> )	$\nu_{(Raman)}$ (cm <sup>-1</sup> )	$\nu_{(Raman)}$ (cm <sup>-1</sup> ) SERS	Assignments
$\nu$ (cm <sup>-1</sup> )	IR intensity	$\nu$ (cm <sup>-1</sup> )	IR intensity	$\nu$ (cm <sup>-1</sup> )	IR intensity				
3620	111.29	3640	7.69	3556	56.69				$\nu$ OH
3433	106.00	3400	56.57	3433	99.28	3343 sbr	3340 w		$\nu$ NH
3098	8.69	3170	3.47	3160	5.89				$\nu$ CH I
3066	2.42	3156	29.20	3139	1.83				$\nu$ CH I
3051	4.15	3156	18.65	3120	2.35				$\nu$ CH II
3047	1.43	3140	1.42	3119	3.97				$\nu$ CH I
3046	1.92	3139	14.84	3119	2.64	3113 sbr	3087 w		$\nu$ CH II
3007	6.27	3137	0.65	3081	6.26		3077 s		$\nu$ CH II
3006	9.10	3134	1.62	3077	9.44	3046 sbr	3039 w		$\nu$ CH II
2933	2.92	3031	29.09	2999	3.14		2992 w	2975 w	$\nu_{as}$ CH <sub>2</sub>
2869	9.13	3028	3.01	2938	10.07	2942 w	2927 w	2928 s	$\nu_s$ CH <sub>2</sub>
1671	237.67	1692	77.36	1639	166.08	1663 s	1658 w	1651 m	$\nu$ C=O
1628	73.27	1620	18.88	1603	35.34	1626 w	1606 s	1606 w	$\nu$ Ph I
1625	23.80	1606	11.05	1600	47.76				$\nu$ Ph II
1608	108.29	1600	148.72	1593	135.85				$\nu$ Ph I
1602	4.81	1595	3.58	1585	4.16	1588 s	1586 s		$\nu$ Ph II
1551	610.41	1565	95.302	1527	608.47	1555 s	1534 s		$\nu_{as}$ NO <sub>2</sub>
1518	107.71	1515	234.07	1507	89.57	1506 vs	1507m		$\nu$ Ph II
1511	31.81	1500	6.36	1497	25.30			1490 w	$\nu$ Ph I, $\delta$ NH
1458	12.63	1459	36.23	1456	12.31			1460 s	$\delta$ CH <sub>2</sub>
1449	406.65	1440	279.96	1432	213.47	1428 s			$\nu$ Ph I, $\delta$ OH
1415	3.28	1421	7.21	1410	2.56		1419 w	1423 w	$\nu$ Ph II
1393	89.73	1390	259.48	1396	32.43	1391 m		1376 m	$\nu_s$ NO <sub>2</sub>
1334	64.42	1370	53.83	1365	103.28		1362 w		$\nu$ Ph I
1329	25.82	1340	12.34	1325	0.61	1339 s	1335 vvs		$\nu$ Ph II, $\nu$ CN
1318	11.73	1320	18.68	1314	58.70			1312 m	$\nu$ Ph I
1314	692.33	1315	79.99	1309	2.34				$\delta$ CH II
1295	203.60	1308	1.656	1301	63.53				$\omega$ CH <sub>2</sub>
1258	14.00	1275	2.51	1261	174.32	1270 w	1268 s		$\delta$ CH I, $\nu$ (C–O) <sub>n</sub>
1246	2.77	1240	49.91	1233	379.35		1230 m		$\nu$ CN
1224	80.86	1232	16.83	1218	82.10	1225 s			$\nu$ CF, $\delta$ CH II
1217	89.79	1230	0.41	1217	12.17				$\delta$ CH I, $\delta$ NH
1202	2.02	1219	108.31	1209	188.86			1203 m	$\tau$ CH <sub>2</sub>
1192	12.05	1202	42.67	1199	1.10	1200 w	1195 w		$\delta$ CH II
1167	13.14	1194	3.77	1169	81.90				$\delta$ CH I
1158	19.76	1182	31.32	1166	23.71	1162 w	1158 w		$\delta$ CH II, $\rho$ NH
1150	96.69	1132	112.28	1142	143.56				$\delta$ CH I
1106	178.56	1111	70.45	1105	156.78	1119 w	1106 w		$\delta$ CH I, $\nu$ CN
1095	8.45	1089	9.62	1102	12.41	1092 w		1089 w	$\delta$ CH II
1082	65.58	1074	42.60	1071	41.61	1078 m	1079 s		$\delta$ CH I
1057	3.14	1030	0.44	1013	4.25	1019 w		1015 w	$\delta$ CH II
1026	0.14	999	0.06	999	1.21			992 s	$\gamma$ CH I
1017	4.80	992	1.36	959	0.17	968 w			$\gamma$ CH II
1009	2.27	976	1.37	950	2.72		946 w		$\gamma$ CH II
950	75.49	955	13.12	938	19.27	940 m			$\gamma$ CH II
947	16.52	939	11.68	930	6.31		934 w	934 s	$\rho$ CH <sub>2</sub>
943	8.92	913	8.57	909	15.15				$\gamma$ CH I, $\nu$ CC
914	23.58	881	15.81	888	69.40	871 m		894 s	$\gamma$ CH I
910	40.89	871	1.91	862	8.16		869 w		$\delta$ NO <sub>2</sub>
888	31.41	861	20.22	860	7.50				$\gamma$ CH II
869	1.31	855	0.26	830	9.16	833 s	844 m	847 s	Ring breath II
839	52.49	846	6.97	825	0.92				$\gamma$ CH I
826	11.87	828	12.65	820	38.13	814 s	813 s		$\gamma$ CH II
790	105.39	784	1.64	772	67.84	778 m	768 w		$\gamma$ NH
784	55.27	730	1.20	763	0.43				$\omega$ NH, $\gamma$ CH II
769	5.37	720	26.93	762	35.22	744 s	759 w	744 s	$\omega$ NO <sub>2</sub>
727	3.42	718	0.65	719	2.57	722 w	718 w		$\gamma$ Ph I
726	15.18	691	48.24	710	18.87	710 w			$\gamma$ Ph II
720	51.53	644	0.21	690	20.17				$\gamma$ Ph I
683	29.74	637	6.60	672	14.66		680 w	669 w	Ring breath I
643	0.23	605	11.63	641	0.11		638 w		$\delta$ Ph II, $\delta$ C=O
627	0.86	582	11.64	612	3.22	621 w		605 w	$\gamma$ OH
589	13.85	547	14.66	583	11.47				$\delta$ Ph(X) II
568	2.44	537	3.52	560	3.98	570 w		555 m	$\gamma$ Ph I(X)
548	6.28	536	8.19	546	3.92	542 m			$\delta$ Ph I
539	15.79	505	15.41	533	13.45				$\gamma$ Ph II, $\rho$ NO <sub>2</sub>
529	7.68	493	8.69	527	4.44		524 w		$\delta$ Ph II
490	11.54	462	8.64	486	10.87	499 w	484 w		$\gamma$ Ph II, $\gamma$ C=O
461	10.93	457	12.53	455	4.57	475 w			$\gamma$ Ph I(X)
430	3.25	425	0.22	424	6.30	445 w	423 w		$\gamma$ Ph II
425	9.99	407	1.34	419	1.13	417 w			$\gamma$ Ph II
400	5.50	399	21.88	398	3.35		389 w		$\delta$ Ph II
382	16.27	385	86.91	377	11.48		377 m		$\delta$ Ph I

(continued on next page)

Table 1 (continued)

HF/6-31G*		B3PW91/6-31G*		B3LYP/6-31G*		$\nu_{\text{IR}}$ (cm <sup>-1</sup> )	$\nu_{\text{Raman}}$ (cm <sup>-1</sup> )	$\nu_{\text{Raman}}$ (cm <sup>-1</sup> ) SERS	Assignments
$\nu$ (cm <sup>-1</sup> )	IR intensity	$\nu$ (cm <sup>-1</sup> )	IR intensity	$\nu$ (cm <sup>-1</sup> )	IR intensity				
357	1.30	360	0.77	356	32.44		356 w	364 m	$\gamma$ Ph I
356	1.03	340	5.71	353	1.05				$\delta$ Ph II
300	0.93	324	0.22	330	134.08				$\delta$ CF(X)II
284	1.38	300	0.95	297	0.68				$\gamma$ CF(X)II
269	191.07	295	0.57	285	0.24		289 w		$\gamma$ CC(X)II
262	9.33	241	1.10	260	2.71		252 w		$\delta$ CO(X)I
221	8.50	212	0.29	218	3.96		221 m		$\gamma$ CO(X)I
217	4.84	161	1.68	215	1.73				$\delta$ CN(X)II
158	4.11	137	1.97	155	2.43				$\gamma$ CN(X)I
142	1.39	131	2.46	142	1.04		146 w		$\gamma$ CN(X) I
103	2.19	82	0.55	101	1.38		98 s		$\gamma$ CC(X)II

$\nu$  – stretching,  $\delta$  – in-plane bending,  $\gamma$  – out-of-plane bending,  $\tau$  – torsion, s – strong, m – medium, w – weak, v – very, br – broad; Ph I and Ph II – tri and para substituted phenyl rings; X – substituent sensitive; subscript: as – asymmetric, s – symmetric.

ents, the bands tend to shift to some what lower wavenumbers, and the greater the number of substituents on the ring, the broader of the absorption regions [38]. In the case of C=O substitution, the band near 1490 cm<sup>-1</sup> can be very weak [38]. The fifth ring stretching vibration is active near 1315 ± 65 cm<sup>-1</sup>, a region that overlaps strongly with that of the CH in-plane deformation [38]. The sixth ring stretching vibration, the ring breathing mode appears as a weak band near 1000 cm<sup>-1</sup> in mono, 1,3-di- and 1,3,5-tri-substituted benzenes. In the otherwise substituted benzenes, however, this vibration is substituent sensitive and difficult to distinguish from other modes. The ring breathing mode for the para substituted benzenes with entirely different substituents [41] has been reported to be strongly IR active with typical bands in the interval 780–840 cm<sup>-1</sup>. For the title compound, this is confirmed by the band in the IR spectrum at 833 and at 844 cm<sup>-1</sup> in Raman spectrum, which finds support from the computational results. The ring breathing mode of para-substituted benzenes are reported at 804 and 792 cm<sup>-1</sup> experimentally and at 782 and 795 cm<sup>-1</sup> theoretically [49,50]. In asymmetric tri-substituted benzenes, when all the three substituents are light, the wavenumber interval of the breathing mode [41] is between 500 and 600 cm<sup>-1</sup>. When all the three substituents are heavy, the wavenumber appears above 1100 cm<sup>-1</sup>. In the case of mixed substituents, the wavenumber is expected [41] to appear between 600 and 750 cm<sup>-1</sup>. For the title compound the phenyl ring I breathing mode is observed at 672 cm<sup>-1</sup> theoretically.

For para-substituted benzenes, the  $\delta$ CH modes are seen in the range 995–1315 cm<sup>-1</sup> and for tri substituted benzenes these modes are in the range [38] 1290–1050 cm<sup>-1</sup>. In the present case,  $\delta$ CH modes are observed in the range 1019–1270 cm<sup>-1</sup> in the IR spectrum and in the range 1079–1268 cm<sup>-1</sup> in the Raman spectrum. The B3LYP calculations give these modes in the range 1013–1309 cm<sup>-1</sup> and some of the bands are not pure but contain significant contribution from other modes. The out-of-plane CH deformations [38] are observed between 700 and 1000 cm<sup>-1</sup>. Generally the CH out-of-plane deformations with the highest wavenumbers are weaker than those absorbing at lower wavenumbers. The strong  $\gamma$ CH band occurring at 840 ± 50 cm<sup>-1</sup>, is typical for para substituted benzenes [38]. For the title compound, a band is observed at 814 cm<sup>-1</sup> in the IR spectrum. Again according to literature [35,38] a lower  $\gamma$ CH absorbs in the neighborhood of 820 ± 45 cm<sup>-1</sup>, but is much weaker or infrared inactive. The DFT calculation give a  $\gamma$ CH at 763 cm<sup>-1</sup> and no band is experimentally observed for this mode. In the case of tri-substituted benzenes, two  $\gamma$ CH bands are observed at 890 ± 50 and 815 ± 45 cm<sup>-1</sup> in the IR spectrum. The bands observed at 871 (IR) 909 cm<sup>-1</sup> (DFT) are assigned to this modes. The IR bands in the 2855–1887 cm<sup>-1</sup> region and their large broadening support the intra molecular hydrogen bonding between the C=O and OH groups [51].

#### 4.2. SERS spectrum

SERS has been applied as a powerful technique for innovative and extensive analytical applications in surface science, electrochemistry, biology and materials research [52–54]. SERS is already regarded as a valuable method because of its high sensitivity, which enables the detection and spectroscopic study of even single molecules [55]. The vibrational information contained in the SERS spectrum provide the molecular specificity required to characterize the adsorbate–surface interactions, specifically, the orientation of the adsorbed species on the metal surface. The relative intensities from the SERS spectra are expected to differ significantly from normal Raman spectra owing to specific surface selection rules [56]. The surface selection rule suggest that for a molecule adsorbed flat on the silver surface, its out-of-plane vibrational modes will be more enhanced when compared with its in-plane vibrational modes and vice versa when it is adsorbed perpendicular to the surface [56,57]. It is further seen that vibrations involving atoms that are close to the silver surface will be more enhanced when the wavenumber difference between the Raman bands in the normal and SERS spectrum is not more than 5 cm<sup>-1</sup>, the molecular plane is expected to be perpendicular to the silver surface [58].

In the SERS spectrum of the title compound the aromatic CH stretching vibration are absent, which means that the phenyl ring may be somewhat flat on the silver surface [58,59]. It has also been documented in literature [60] that when a benzene ring moiety interacts directly with a metal surface, the ring breathing mode is red shifted by 10 cm<sup>-1</sup> along with substantial band broadening in the SERS spectrum. In the present case, the ring breathing modes of ring I and II are present in the SERS spectrum at 669 cm<sup>-1</sup> and 847 cm<sup>-1</sup>. Neither a substantial red shift nor a significant band broadening was observed in the SERS spectrum, for the Phenyl ring II where as, for the phenyl ring I, the ring breathing mode is red shifted by 11 cm<sup>-1</sup> imply that the probability of a direct ring  $\pi$ -orbital of phenyl ring I to metal surface is present. The presence of CH<sub>2</sub> modes 2975, 2928, 1460, 1203, 934 cm<sup>-1</sup> in the SERS spectrum indicates the closeness of CH<sub>2</sub>–C=O group with metal surface and interaction of the silver surface with this moiety. This is supported by the presence of  $\nu$ C=O band at 1651 cm<sup>-1</sup> in the SERS spectrum

The in-plane bending modes  $\delta$ CH of the phenyl ring I are not observed in the SERS spectrum whereas for phenyl ring II, the  $\delta$ CH modes are observed at 1089 and 1015 cm<sup>-1</sup> which are absent in the normal Raman spectrum. The presence of these modes suggest that the benzene ring II is oriented tilted to the silver surface [56,57]. The phenyl ring stretching vibrations are observed at 1606, 1490, 1312 cm<sup>-1</sup> for Ph I and at 1423 cm<sup>-1</sup> for PhII in the SERS spectrum. The out-of-plane CH deformations of phenyl ring I are present in the SERS spectrum at 992, 894 cm<sup>-1</sup> which are ab-

sent in the normal Raman spectrum whereas  $\gamma$ CH of Ph II are absent in the SERS spectrum of the title compound.

In the SERS spectrum of 2-amino-5-nitropyridine [61] the symmetric NO<sub>2</sub> stretching mode corresponds to the most intense band, which appears broad and significantly down shifted from 1344 cm<sup>-1</sup> to 1326 cm<sup>-1</sup> suggesting binding to silver through the lone pairs of the oxygen atom. Carrasco et al. [62] observed the NO<sub>2</sub> stretch in the SERS spectrum at ~1500 cm<sup>-1</sup> with medium intensity, which demonstrated the importance of nitro group in regard to the interaction with the metal surface. Further, they observed the enhancement of  $\nu$ Ph modes, revealing that the molecule is oriented perpendicular to the metal surface, whereas the changes that occur in the nitro group indicate that the interaction occurs through oxygen atoms of the nitro moiety. The interaction induces a  $\pi$ -electronic redistribution primarily around both the nitro group and the aromatic portion in the vicinity of the substitution site. Also Gao and Weaver [63] observed broadening and a downshift of the corresponding band of nitrobenzene adsorbed on gold via nitro group. For the title compound the symmetric stretching mode of NO<sub>2</sub> which is absent in the normal Raman spectrum appears at 1376 cm<sup>-1</sup> in the SERS spectrum. Interaction through the NO<sub>2</sub> group was also supported by the presence of mode at 744 cm<sup>-1</sup>.

Keeping in mind the behavior observed for molecules containing  $\pi$ -system adsorbed flat on the metal surface [57,63–65], a purely parallel orientation of the molecular skeleton with respect to the surface appears unlikely in the light of the following arguments. The ring breathing modes of phenyl ring II appears as a strong band at 847 cm<sup>-1</sup> without any significant band broadening or red shift where as for phenyl ring I, a weak SERS band is observed at 669 cm<sup>-1</sup> with a red shift of 11 cm<sup>-1</sup>. Also in-plane  $\delta$ CH modes of Ph I are absent in the SERS spectrum while for Ph II  $\delta$ CH modes are present in the SERS spectrum. The  $\gamma$ CH modes of Ph I are present in the SERS spectrum while that of Ph II are absent. The substituent sensitive modes of Phenyl ring I are in present in the SERS spectrum at 555 and 364 cm<sup>-1</sup>. The  $\nu$ Ph modes of Ph I and Ph II are also present in the SERS spectrum. The appearance of these modes support that both the ring are tilted with respect to the metal surface [58,59,66].

#### 4.3. Geometrical parameters and first hyperpolarizability

To best of our knowledge, no X-ray crystallographic data of this molecule have yet been reported. However, the theoretical results obtained are almost comparable with the reported structural parameters of similar derivatives. The carbon–oxygen (phenolate) C<sub>13</sub>–O<sub>28</sub> distance is 1.3940 Å where as the average CO bond length is 1.362 for phenols [67]. B3LYP calculations give shortening of the angles C<sub>14</sub>–C<sub>17</sub>–N<sub>30</sub> by 0.2°, C<sub>16</sub>–C<sub>17</sub>–N<sub>30</sub> by 1.5° at C<sub>17</sub> position, C<sub>17</sub>–N<sub>30</sub>–O<sub>32</sub> by 1.7°, C<sub>17</sub>–N<sub>30</sub>–O<sub>31</sub> by 2° at N<sub>30</sub> position from 120°. This reduction in angles reveal the hydrogen bonding between H<sub>18</sub> and H<sub>19</sub> atoms, which is evident from the enlargement in the angles C<sub>14</sub>–C<sub>17</sub>–C<sub>16</sub> by 1.8 and O<sub>31</sub>–N<sub>30</sub>–O<sub>32</sub> by 3.6° from 120°. The bond angles of the NO<sub>2</sub> group of the title compound O<sub>32</sub>–N<sub>30</sub>–O<sub>31</sub> = 123.6°, O<sub>32</sub>–N<sub>30</sub>–C<sub>17</sub> = 118.3° and O<sub>31</sub>–N<sub>30</sub>–C<sub>17</sub> = 118.0° which are in agreement with the values 123.5, 118.7 and 117.9° given by Saeed et al. [68].

For Benzamide derivatives, Noveron et al. [69] reported the bond lengths C<sub>11</sub>–N<sub>26</sub>, C<sub>24</sub>–O<sub>25</sub>, C<sub>24</sub>–N<sub>26</sub>, C<sub>24</sub>–C<sub>21</sub> and N<sub>26</sub>–H<sub>27</sub> as 1.3953, 1.2253, 1.3703, 1.4943 and 0.733 Å, where as the corresponding values for the title compound are, 1.3998, 1.2478, 1.3801, 1.5340 and 1.0144 Å. For N-(2-pyridyl)benzamide complexes [70] the bond lengths C<sub>24</sub>–O<sub>25</sub> = 1.2445, C<sub>24</sub>–N<sub>26</sub> = 1.3646, C<sub>11</sub>–N<sub>26</sub> = 1.4156 Å and for the title compounds the corresponding values are 1.2478, 1.3801 and 1.3998 Å. The C=O and C=N bond lengths [16] in benzamide, acetamide and formamide are respectively, 1.2253, 1.2203, 1.2123 and 1.3801, 1.3804, 1.3683 Å. According

to literature [8,10,14,71] the changes in bond lengths in C=O and C–N are consistent with the following interpretation: that is, hydrogen bond decreases the double bond character of C=O bond and increases the double bond character of C–N bond. For 2-nitro-N-(4-nitrophenyl)benzamide [68] C<sub>24</sub>–O<sub>25</sub> = 1.2132, N<sub>30</sub>–O<sub>32</sub> = 1.2292, N<sub>30</sub>–O<sub>31</sub> = 1.2252, N<sub>26</sub>–C<sub>24</sub> = 1.3612, N<sub>26</sub>–C<sub>11</sub> = 1.4042 and N<sub>30</sub>–C<sub>17</sub> = 1.4632 Å. The B3LYP calculations give the corresponding values as 1.2478, 1.2658, 1.2687, 1.3801, 1.3998 and 1.4556 Å for the title compound. For the benzamide moiety of the title compound the calculated values of the bond angles C<sub>24</sub>–N<sub>26</sub>–C<sub>11</sub>, C<sub>13</sub>–C<sub>11</sub>–N<sub>26</sub>, O<sub>25</sub>–C<sub>24</sub>–N<sub>26</sub>, O<sub>2</sub>–C<sub>24</sub>–C<sub>21</sub>, N<sub>26</sub>–C<sub>24</sub>–C<sub>21</sub> are 127.9, 115.9, 123.7, 120.7, 115.5° whereas the reported values of similar derivatives are 124.7, 116.6, 123.1, 118.7, 118.3° [70] and 122.7, 120.3, 122.1, 122.7, 115.2° [72]. In the present case, at C<sub>24</sub> position the angles C<sub>21</sub>–C<sub>24</sub>–O<sub>25</sub> = 120.7°, C<sub>26</sub>–C<sub>24</sub>–O<sub>25</sub> = 123.7° and C<sub>26</sub>–C<sub>24</sub>–C<sub>21</sub> = 115.5° and this asymmetry of exocyclic angles reveals the interaction between O<sub>25</sub> and H<sub>23</sub>.

Also at C<sub>11</sub> position the angles C<sub>12</sub>–C<sub>11</sub>–N<sub>26</sub> is increased by 5.1° and C<sub>13</sub>–C<sub>11</sub>–N<sub>26</sub> is reduced by 4.1° from 120° and this asymmetry reveals the interaction between the amide moiety and the phenyl ring I. The CC bond lengths in the phenyl ring I lie between 1.3837–1.4181 Å, whereas for the phenyl ring II, the range is 1.3895–1.4084 Å. The CH bond lengths lie between 1.0794 and 1.0830 Å for phenyl ring I and 1.0830 and 1.0860 Å for phenyl ring II. The CC bond length of benzene [73] is 1.3993 Å and benzaldehyde [74] is 1.3973 Å. The torsion angles around the benzamide group in the present case C<sub>14</sub>–C<sub>12</sub>–C<sub>11</sub>–N<sub>26</sub> = –179.9, N<sub>26</sub>–C<sub>11</sub>–C<sub>13</sub>–C<sub>16</sub> = 179.9, O<sub>25</sub>–C<sub>24</sub>–C<sub>21</sub>–C<sub>3</sub> = –153.7, N<sub>26</sub>–C<sub>24</sub>–C<sub>21</sub>–C<sub>3</sub> = 28.8 where as the corresponding reported values are 178.5, –178.9, 161.1163.8 [69] and –178.3, –179.8, –158.2, 22.1 [72]. The strong steric repulsion between phenyl ring II and the amide group is confirmed by the non-planarity of the benzamide, where the amide group is turned by –153.7 (C<sub>3</sub>–C<sub>21</sub>–C<sub>24</sub>–O<sub>25</sub>), and 77.3 (C<sub>2</sub>–C<sub>3</sub>–C<sub>21</sub>–C<sub>24</sub>) with respect to the benzene ring [14]. That is, it may be due to the repulsion between hydrogen atoms H<sub>8</sub> and H<sub>23</sub> as reported in literature [13,14,16,73].

The values of angles C<sub>3</sub>–C<sub>21</sub>–C<sub>24</sub> 116.6 and C<sub>21</sub>–C<sub>24</sub>–O<sub>25</sub> 120.7° of the benzamide group of the title compound are smaller than those of benzaldehyde (120.6 and 123.6°) [74]. These differences are ascribed to the steric repulsion between H<sub>23</sub> and H<sub>22</sub> atoms. The C<sub>21</sub>–C<sub>24</sub> bond length 1.5340 is larger than the corresponding length of benzaldehyde [74] (1.4794 Å) by about 0.0546 Å. The C<sub>24</sub>–O<sub>25</sub> bond length 1.2478 Å given by B3LYP calculation is greater than that of a similar benzamide by 0.0025 Å, where the C<sub>24</sub>–N<sub>26</sub> bond length 1.3801 is larger by 0.0191 Å [16]. The corresponding difference for acetamide are 0.03 and 0.04 Å and those for formamide are 0.03 and 0.05. The changes found for benzamide are similar to those for formamide [6] and acetamide [7,8,11]. The C<sub>3</sub>–C<sub>21</sub> bond length 1.5149 Å is also shorter than reported values of similar molecules [16], although the difference is not large as the difference in the C=O and C–N bonds. This shortening indicates that the conjugation between amide group and phenyl groups increases in the crystal.

For benzamide derivatives, Nishikawa et al. [20] reported the bond lengths C<sub>21</sub>–C<sub>24</sub> = 1.489–1.505, C<sub>24</sub>–O<sub>25</sub> = 1.211–1.226, C<sub>24</sub>–N<sub>26</sub> = 1.37–1.388, N<sub>26</sub>–H<sub>27</sub> = 1.01, N<sub>26</sub>–C<sub>11</sub> = 1.396–1.411 Å, the bond angles, C<sub>21</sub>–C<sub>24</sub>–O<sub>25</sub> = 121.3–124.7, O<sub>25</sub>–C<sub>24</sub>–N<sub>26</sub> = 123.0–123.8, C<sub>24</sub>–N<sub>26</sub>–H<sub>27</sub> = 115.9–116.0, C<sub>24</sub>–N<sub>26</sub>–C<sub>11</sub> = 121.0–129.0, H<sub>27</sub>–N<sub>26</sub>–C<sub>11</sub> = 114.7 and the dihedral angles, C<sub>3</sub>–C<sub>21</sub>–C<sub>24</sub>–O<sub>25</sub> = –1.1–23.92, O<sub>25</sub>–C<sub>24</sub>–N<sub>26</sub>–C<sub>11</sub> = 0.6–2.8, O<sub>25</sub>–C<sub>24</sub>–N<sub>26</sub>–H<sub>27</sub> = 170.5–171.6, H<sub>27</sub>–N<sub>26</sub>–C<sub>11</sub>–C<sub>12</sub> = –178.0, C<sub>24</sub>–N<sub>26</sub>–C<sub>11</sub>–C<sub>12</sub> = 4.5–49.1°. In the present case, the corresponding calculated values are 1.5340, 1.2478, 1.3801, 1.0144, 1.3998 Å (bond lengths), 120.7°, 123.7°, 117.7°, 127.9°, 114.5° (bond angles) and –153.7°, –0.5°, 178.1°, –178.7°, –0.1° (dihedral angles). Zhou

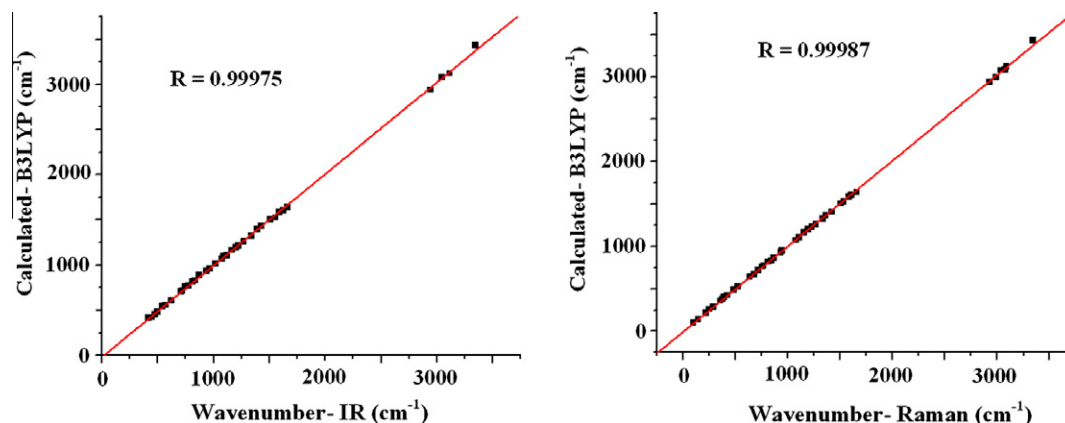


Fig. 8. Correlation graph.

et al. [75] reported  $O_{25}-C_{24} = 1.2723^\circ$  (XRD), 1.249 (DFT),  $N_{26}-C_{11} = 1.3443$  (XRD) 1.414 (DFT),  $N_{26}-C_{24} = 1.3193$  (XRD), 1.399 (DFT),  $C_{21}-C_{24}-O_{25} = 115.1$  (XRD), 118.0 (DFT),  $C_{21}-C_{24}-N_{26} = 115.2$  (XRD), 123.9° (DFT) for a similar benzamide derivative, which is in agreement with our calculated values, 1.2478°, 1.3998°, 1.3801°, 120.7° and 115.5°.

For 2-hydroxy-benzamides, Kawski et al. [4] reported the bond lengths,  $O_{28}-C_{13} = 1.3634$ ,  $O_{25}-C_{24} = 1.2553$ ,  $N_{26}-C_{24} = 1.3334$ ,  $C_3-C_{21} = 1.5044$ ,  $N_{26}-C_{11} = 1.4634$  Å whereas the corresponding calculated values for the title compound are 1.3940, 1.2478, 1.3801, 1.5149, 1.3998 Å. In the present case, the bond angles,  $O_{28}-C_{13}-C_{11} = 114.9$ ,  $O_{28}-C_{13}-C_{16} = 123.7$ ,  $C_{11}-C_{13}-C_{16} = 121.4$ ,  $O_{25}-C_{24}-N_{26} = 123.7$ ,  $O_{25}-C_{24}-C_{21} = 120.7$ ,  $N_{26}-C_{24}-C_{21} = 115.5$ ,  $C_{24}-N_{26}-C_{11} = 127.9$ ,  $N_{26}-C_{11}-C_{13} = 115.9$  whereas the reported values are 117.8, 121.7, 120.5, 121.1, 119.7, 119.1, 124.6, 112.1° [4].

Analysis of organic molecules having conjugated  $\pi$ -electron systems and large hyperpolarizability using infrared and Raman spectroscopy has evolved as a subject of research [76]. The potential application of the title compound in the field of nonlinear optics demands the investigation of its structural and bonding features contributing to the hyperpolarizability enhancement, by analyzing the vibrational modes using the IR and Raman spectrum. The ring stretching bands at 1626, 1588, 1506, 1339, 833  $cm^{-1}$  observed in IR have their counterparts in the Raman spectrum at 1606, 1586, 1506, 1335, 844  $cm^{-1}$ , respectively and their relative intensities in IR and Raman spectrum are comparable. The first hyperpolarizability ( $\beta_0$ ) of this novel molecular system is calculated using DFT method, based on the finite field approach. In the presence of an applied electric field, the energy of a system is a function of the electric field. First hyperpolarizability is a third rank tensor that can be described by a  $3 \times 3 \times 3$  matrix. The 27 components of the 3D matrix can be reduced to 10 components due to the Kleinman symmetry [77]. The components of  $\beta$  are defined as the coefficients in the Taylor series expansion of the energy in the external electric field. When the electric field is weak and homogeneous, this expansion becomes

$$E = E_0 - \sum_i \mu_i F^i - \frac{1}{2} \sum_{ij} \alpha_{ij} F^i F^j - \frac{1}{6} \sum_{ijk} \beta_{ijk} F^i F^j F^k - \frac{1}{24} \sum_{ijkl} \gamma_{ijkl} F^i F^j F^k F^l + \dots$$

where  $E_0$  is the energy of the unperturbed molecule,  $F^i$  is the field at the origin,  $\mu_i$ ,  $\alpha_{ij}$ ,  $\beta_{ijk}$  and  $\gamma_{ijkl}$  are the components of dipole moment, polarizability, the first hyper polarizabilities, and second hyperpolarizabilities, respectively. The calculated first hyperpolarizability of the title compound is  $9.432 \times 10^{-30}$  esu, which is comparable with the reported values of similar derivatives [72] which is 42 times the corresponding value for the standard NLO material urea

[78]. We conclude that the title compound is an attractive object for future studies of nonlinear optical properties.

In order to investigate the performance and vibrational wavenumbers of the title compound root mean square (RMS) value and correlation coefficients between calculated and observed wavenumbers were calculated (Fig. 8). RMS values of wavenumbers were evaluated using the following expression [3].

$$RMS = \sqrt{\frac{1}{n-1} \sum_i^n (v_i^{calc} - v_i^{exp})^2}$$

The RMS error of the observed Raman bands and IR bands are found to be 32.12, 35.01 for HF, 24.69, 26.09 for B3PW91 and 12.03, 14.01 for B3LYP methods, respectively. The small differences between experimental and calculated vibrational modes are observed. It must be due to the fact that hydrogen bond vibrations present in the crystal lead to strong perturbation of the infrared wavenumbers and intensities of many other modes. Also, we state that experimental results belong to solid phase and theoretical calculations belong to gaseous phase.

## 5. Conclusion

The FT-IR, FT-Raman and SERS spectra of 4-fluoro-N-(2-hydroxy-4-nitrophenyl) phenylacetamide were studied. The molecular geometry and the wavenumbers were calculated using different levels of theory. The observed wavenumbers are found to be in agreement with the calculated (B3LYP) values. The presence of  $CH_2$  and  $NO_2$  modes in the SERS spectrum indicates the nearness of these groups to the metal surface, which affects the orientation and metal molecule interaction. The presence of phenyl ring deformation bands, show a tilted orientation of the molecule with respect to the silver surface. The red shift of the NH stretching wavenumber in the IR spectrum from the calculated wavenumber indicates the weakening of NH bond resulting in proton transfer to the neighboring oxygen atom. The geometrical parameters of the title compound are in agreement with the reported similar derivatives.

## Appendix A. Supplementary material

Supplementary data associated with this article can be found, in the online version, at doi:10.1016/j.molstruc.2011.03.022.

## References

- [1] E.A. Sener, K.K. Bingol, I. Oren, O.T. Arpaci, I. Yalcin, N. Altanlar, *Farmaco* 55 (2000) 469.
- [2] E. Aki-Sener, K.K. Bingol, O. Temiz-Arpaci, I. Yalcin, N. Altanlar, *Farmaco* 57 (2002) 451.

- [3] L. Ushakumari, H.T. Varghese, C.Y. Panicker, T. Ertan, I. Yildiz, J. Raman Spectrosc. 39 (2008) 1832.
- [4] P. Kawski, A. Kochel, M.G. Perevozkina, A. Filarowski, J. Mol. Struct. 790 (2006) 65.
- [5] H. Arslan, U. Florke, N. Kulcu, G. Binzet, Spectrochim. Acta 68A (2007) 1347.
- [6] M. Kitano, K. Kuchitsu, Bull. Chem. Soc. Jpn. 47 (1974) 67.
- [7] M. Kitano, K. Kuchitsu, Bull. Chem. Soc. Jpn. 46 (1973) 3048.
- [8] E.D. Stevens, Acta Cryst. 34B (1978) 544.
- [9] J. Ladell, B. Post, Acta Cryst. 7 (1954) 559.
- [10] T. Ottersen, Acta Chem. Scand. 29A (1975) 939.
- [11] G.A. Jeffrey, J.R. Ruble, R.K. McMullan, D.F. DeFrees, J.S. Binkley, J.A. Pople, Acta Cryst. 36B (1980) 2292.
- [12] W.A. Denne, R.W.H. Small, Acta Cryst. 27B (1971) 1094.
- [13] C.C.F. Blake, R.W.H. Small, Acta Cryst. 28B (1972) 2201.
- [14] Q. Gao, G.A. Jeffrey, J.R. Ruble, R.K. McMullan, Acta Cryst. 47B (1991) 742.
- [15] Y.S. Choi, J. Kim, J. Park, J. Yu, C. Yoon, Spectrochim. Acta 52A (1996) 1779.
- [16] H. Takeuchi, M. Sato, T. Tsuji, H. Takashima, T. Egawa, S. Konaka, J. Mol. Struct. 485–486 (1999) 175.
- [17] G. Biagi, I. Giorgi, O. Livi, A. Nardi, V. Calderone, A. Martelli, E. Martinotti, O.L. Salerno, Eur. J. Med. Chem. 39 (2004) 491.
- [18] H.S. Rho, H.S. Baek, S.M. Ahn, J.W. Yoo, D.H. Kim, H.G. Kim, Bioorg. Med. Chem. Lett. 19 (2009) 1532.
- [19] H.A. Dabbagh, A. Teimouri, A.N. Chermahini, M. Shahraki, Spectrochim. Acta 69A (2008) 449.
- [20] J. Nishikawa, T. Imase, M. Koike, K. Fukuda, M. Tokita, J. Watanabe, S. Kawauchi, J. Mol. Struct. 741 (2005) 221.
- [21] Y.R. Shen, The Principles of Nonlinear Optics, Wiley, New York, 1984.
- [22] P.V. Kolinsky, Opt. Eng. 31 (1992) 1676.
- [23] D.F. Eaton, Science 253 (1991) 281.
- [24] C.R. Moylan, R.J. Twieg, V.Y. Lee, S.A. Swanson, K.M. Betterton, R.D. Miller, J. Am. Chem. Soc. 115 (1993) 12599.
- [25] S. Gilmour, R.A. Montgomery, S.R. Marder, L.T. Cheng, A.K.Y. Je, Y. Cai, J.W. Perry, L.R. Dalton, Chem. Mater. 6 (1994) 1603.
- [26] C. Ravikumar, I.H. Joe, V.S. Jayakumar, Chem. Phys. Lett. 460 (2008) 552.
- [27] T. Ertan, I. Yildiz, S. Ozkan, O.T. Arpacı, F. Kaynak, I. Yalcin, E.A. Sener, U. Abbasoglu, Bioorg. Med. Chem. 15 (2007) 2032.
- [28] P.C. Lee, D.J. Meisel, J. Phys. Chem. 86 (1982) 3391.
- [29] M.J. Frisch, G.W. Trucks, H.B. Schlegel, G.E. Scuseria, M.A. Robb, J.R. Cheeseman, J.A. Montgomery, Jr., T. Vreven, K.N. Kudin, J.C. Burant, J.M. Millam, S.S. Iyengar, J. Tomasi, V. Barone, B. Mennucci, M. Cossi, G. Scalmani, N. Rega, G.A. Petersson, H. Nakatsuji, M. Hada, M. Ehara, K. Toyota, R. Fukuda, J. Hasegawa, M. Ishida, T. Nakajima, Y. Honda, O. Kitao, H. Nakai, M. Klene, X. Li, J.E. Knox, H.P. Hratchian, J.B. Cross, C. Adamo, J. Jaramillo, R. Gomperts, R.E. Stratmann, O. Yazyev, A.J. Austin, R. Cammi, C. Pomelli, J.W. Ochterski, P.Y. Ayala, K. Morokuma, G.A. Voth, P. Salvador, J.J. Dannenberg, V.G. Zakrzewski, S. Dapprich, A.D. Daniels, M.C. Strain, O. Farkas, D.K. Malick, A.D. Rabuck, K. Raghavachari, J.B. Foresman, J.V. Ortiz, Q. Cui, A.G. Baboul, S. Clifford, J. Cioslowski, B.B. Stefanov, G. Liu, A. Liashenko, P. Piskorz, I. Komaromi, R.L. Martin, D.J. Fox, T. Keith, M.A. Al-Laham, C.Y. Peng, A. Nanayakkara, M. Challacombe, P.M.W. Gill, B. Johnson, W. Chen, M.W. Wong, C. Gonzalez, J.A. Pople, Gaussian 03, Revision C.02, Gaussian, Wallingford, 2004.
- [30] J.B. Foresman, in: E. Frisch (Ed.), Exploring Chemistry with Electronic Structure Methods: A Guide to Using Gaussian, Gaussian, Pittsburg, PA, 1996.
- [31] A.P. Scott, L. Radom, J. Phys. Chem. 100 (1996) 16503.
- [32] G. Rauhut, P. Pulay, J. Phys. Chem. 99 (1995) 3093.
- [33] P. Flukiger, H.P. Luthi, S. Portmann, J. Weber, MOLEKEL, 4.3, Swiss Center for Scientific Computing, Manno, Switzerland, 2000.
- [34] S. Portmann, H.P. Luthi, Chimia 54 (2000) 766.
- [35] N.B. Colthup, L.H. Daly, S.E. Wiberly, Introduction to Infrared and Raman Spectroscopy, third ed., Academic Press, Boston, 1990.
- [36] R. Saxena, L.D. Kaudpal, G.N. Mathur, J. Polym. Sci. Part A: Polym. Chem. 40 (2002) 3959.
- [37] P.L. Anto, C.Y. Panicker, H.T. Varghese, D. Philip, O. Temiz-Arpaci, B.T. Gulbas, I. Yildiz, Spectrochim. Acta 67A (2007) 744.
- [38] N.P.G. Roeges, A Guide to the Complete Interpretation of Infrared Spectra of Organic Structures, Wiley, New York, 1994.
- [39] M. Barthes, G. De Nunzio, G. Riber, Synth. Met. 76 (1996) 337.
- [40] A.S. El-Shahawy, S.M. Ahmed, N.K. Sayed, Spectrochim. Acta 66A (2007) 143.
- [41] G. Varsanyi, Assignments of Vibrational Spectra of Seven Hundred Benzene Derivatives, Wiley, New York, 1974.
- [42] G. Varsanyi, P. Sohar, Acta Chim. Acad. Sci. Hung. 76 (1973) 243.
- [43] A. Perjessy, D. Rasala, P. Tomasik, R. Gawinecki, Collect. Czech. Chem. Commun. 50 (1985) 244.
- [44] J.F. Brown Jr., J. Am. Chem. Soc. 77 (1955) 6341.
- [45] J.H.S. Green, V. Kynaston, A.S. Lindsery, Spectrochim. Acta 17 (1961) 486.
- [46] O. Exner, S. Kovac, E. Sokaniova, Collect. Czech. Chem. Commun. 37 (1972) 2156.
- [47] D.S.R. Rao, G. Thyagarajan, Indian J. Pure Appl. Phys. 16 (1978) 941.
- [48] N. Sundaraganesan, S. Ayyappan, H. Umamaheswari, B.D. Joshua, Spectrochim. Acta 66A (2007) 17.
- [49] Y.S. Mary, H.T. Varghese, C.Y. Panicker, T. Ertan, I. Yildiz, O. Temiz-Arpaci, Spectrochim. Acta 71 (2008) 566.
- [50] A.R. Ambujakshan, V.S. Madhavan, H.T. Varghese, C.Y. Panicker, O. Temiz-Arpaci, B.T. Gulbas, I. Yildiz, Spectrochim. Acta 69A (2007) 782.
- [51] D. Philip, A. John, C.Y. Panicker, H.T. Varghese, Spectrochim. Acta 57 (2001) 1561.
- [52] W.B. Cai, T. Amano, M. Osawa, J. Electroanal. Chem. 500 (2001) 147.
- [53] K. Kneipp, H. Kneipp, I. Itzkan, R.R. Dasari, M.S. Feld, Chem. Rev. 99 (1999) 2957.
- [54] V. Oklejas, C. Sjostrom, J.M. Harris, J. Am. Chem. Soc. 124 (2002) 2408.
- [55] S. Nie, S.R. Emory, Science 275 (1997) 1102.
- [56] J.A. Creighton, Spectroscopy of Surfaces – Advances in Spectroscopy, vol. 16, Wiley, New York, 1988, p. 37 (Chapter 2).
- [57] X. Gao, J.P. Davies, M.J. Weaver, J. Phys. Chem. A 94 (1990) 6858.
- [58] G. Levi, J. Patigny, J.P. Massault, J. Aubard, in: Thirteenth International Conference on Raman Spectroscopy, Wurzburg, 1992, p. 652.
- [59] J.S. Suh, M. Moskovits, J. Am. Chem. Soc. 108 (1986) 4711.
- [60] P. Cao, M.J. Weaver, J. Phys. Chem. A 93 (1989) 6205.
- [61] M.M. Maurizio, Vib. Spectrosc. 29 (2002) 229.
- [62] E.A. Carrasco, F.M. Compos-Vallette, P. Leyton, G. Diaz, R.E. Clavijo, J.V. Garcia-Ramos, N. Inostroza, C. Domingo, S. Sanchez-Cortes, R. Koch, J. Phys. Chem. 107 (2003) 9611.
- [63] P. Gao, M.J. Weaver, J. Phys. Chem. 89 (1985) 5040.
- [64] M.L. Patterson, M.J. Weaver, J. Phys. Chem. 89 (1985) 5046.
- [65] Y.J. Kwon, D.H. Son, S.I. Ahn, M.S. Kim, S. Kim, J. Phys. Chem. 98 (1994) 8481.
- [66] J.A. Creighton, Surf. Sci. 124 (1983) 209.
- [67] F.H. Allen, O. Kennard, D.G. Watson, L. Brammer, A.G. Orpen, R. Taylor, J. Chem. Soc. Perkin Trans. 2 (1987) 51.
- [68] A.S. Saeed, S. Hussain, U. Florke, Turk. J. Chem. 32 (2008) 1.
- [69] J.C. Noveron, A.M. Arif, P.J. Stang, Chem. Mater. 15 (2003) 372.
- [70] W.H. Sun, W. Zhang, T. Gao, X. Tang, L. Chen, Y. Li, X. Jin, Organomet. Chem. 689 (2004) 917.
- [71] J.L. Katz, B. Post, Acta Cryst. 13 (1960) 624.
- [72] C.Y. Panicker, H.T. Varghese, L. Ushakumari, T. Ertan, I. Yildiz, C.M. Granadeiro, H.I.S. Nogueira, Y.S. Mary, J. Raman Spectrosc. 41 (2010) 381.
- [73] K. Tamagawa, T. Iijima, M. Kimura, J. Mol. Struct. 30 (1976) 243.
- [74] K.B. Borizenko, C.W. Bock, I. Hargittai, J. Phys. Chem. 100 (1996) 7426.
- [75] W. Zhou, L. Zhu, Y. Zhang, Z. Yu, L. Lu, X. Yang, Vib. Spectrosc. 36 (2004) 73.
- [76] M. Tommasini, C. Castiglioni, M. Del Zoppo, G. Zerbi, J. Mol. Struct. 480 (1999) 179.
- [77] D.A. Kleinman, Phys. Rev. 126 (1962) 1977.
- [78] M. Adant, I. Dupuis, L. Bredas, Int. J. Quantum. Chem. 56 (2004) 497.